Geotextiles and Geomembranes 47 (2019) 255–268

Contents lists available at ScienceDirect

Geotextiles and Geomembranes

journal homepage: www.elsevier.com/locate/geotexmem

Water retention of geosynthetics clay liners: Dependence on void ratio and temperature

Ali Ghavam-Nasiri[a,*], Abbas El-Zein[a], David Airey[a], R. Kerry Rowe[b]

[a] School of Civil Engineering, The University of Sydney, Australia
[b] Canada Research Chair in Geotechnical and Geoenvironmental Engineering, GeoEngineering Centre at Queen's–RMC, Queen's Univ., Ellis Hall, Kingston, Canada

ARTICLE INFO

Keywords:
Geosynthetics
Void ratio and temperature-dependent SWCC
GCL
Composite lining systems

ABSTRACT

The dependence of the geosynthetic clay liners (GCLs) soil-water characteristic curve (SWCC) on temperature and overburden stress are characterised experimentally. It is shown that changes in void ratio and temperature alter the relationship between suction and moisture content and new forms of existing SWCC equations are developed. To cover a wide suction range, the SWCCs are measured using axis-translation and dew point methods. Based on the available experimental data, both proposed SWCCs are shown to perform well in predicting the effects of void ratio on SWCC along the drying path when compared to the experimental results. It is found that the air-entry value increases as the net vertical stress increases for the experiments under the same temperature. In addition, elevation of temperature reduces retention capacity of the GCL.

1. Introduction

Geosynthetic clay liners are widely used to protect the environment from contamination, especially groundwater (Rowe, 2012). GCLs, commonly comprised of a layer of sodium bentonite between two layers of geotextile and held together by needle-punching (Rowe et al., 2004), usually hydrate from the subgrade and operate under unsaturated conditions. In general, their initial gravimetric water content is very low (typically less than 10%), and they rarely reach full saturation even when properly hydrated by the subsoil. GCLs can undergo a notable increase in water content and achieve a relatively high void ratio under low stresses. This is important for their performance since, without hydration from the subsoil, GCLs would not achieve the swelling and associated low hydraulic conductivities required in liner designs. Understanding hydration dynamics of GCLs and the effects of subsoil properties such as particle size and mineralogy are therefore critical (Bouazza et al., 2017). In addition, GCLs, used as part of composite bottom liners, are often exposed to significant temperature increases in applications such as landfills with maximum temperatures of 55–70 °C (Southen and Rowe, 2005; Yeşiller et al., 2005; Jafari et al., 2014), and brine ponds with maximum temperatures of 70–90 °C (Leblanc et al., 2011; Bouazza et al., 2014; Rowe and Shoaib, 2017). Hence, a thermo-hydro-mechanical (THM) theory for unsaturated porous media is required to describe the complex behaviour of these lining systems.

A key constitutive equation in unsaturated soil mechanics is the relationship between water content and suction, known as soil-water characteristic curve (SWCC). The SWCC of a GCL is important in determining its hydraulic behaviour, volume change, and strength. These factors are essential in evaluating the performance of GCLs as a hydraulic barrier for two main reasons: 1) predicting the extent and rate of hydration from the subsoil and 2) assessing the risk of desiccation of GCLs under thermal gradients. It has been well-established that the SWCC of a porous media alters as a result of changes in volume (e.g. Khalili et al., 2008; Tarantino, 2009; Gallipoli, 2012; Russell, 2014; Huang et al., 2016) and changes in temperature (e.g. Romero et al., 2001; Ye et al., 2009; Zhou et al., 2014; Gao and Shao, 2015; Roshani and Sedano, 2016). Therefore, it is important to consider these effects on the SWCC of GCLs.

2. Background

The range of suctions in a GCL is wide and this necessitates a number of different methods to measure or estimate the SWCCs of GCLs. Experiments on different soils show that soil suction can vary from zero at a fully saturated state to hundreds of MPa at an oven-dry state (105 °C) (Wang et al., 2016). Measuring SWCCs over the entire range of suctions in a GCL is a challenging task. The composite structure of the GCL and the possibility of capillary breakage because of the

* Corresponding author.
E-mail addresses: ali.ghavam-nasiri@sydney.edu.au (A. Ghavam-Nasiri), abbas.el-zein@sydney.edu.au (A. El-Zein), david.airey@sydney.edu.au (D. Airey), kerry.rowe@queensu.ca (R.K. Rowe).

https://doi.org/10.1016/j.geotexmem.2018.12.014
Received 11 July 2018; Received in revised form 25 November 2018; Accepted 22 December 2018
0266-1144/

presence of cover and carrier geotextiles considerably reduces the range of applicability of direct methods to measure suction. For example, Hanson et al. (2013), limited their measurements of the axis-translation method to suctions from 0 to 300 kPa. In addition (Southen and Rowe, 2007), reported scattered measurements of matric suction because of poor contact and capillary breaks for suctions higher than 1 MPa using the axis-translation method.

The SWCC of a GCL was studied by Barroso and Touze-Foltz (2006) using the contact filter paper (CFP) method. Both CFP and non-contact filter paper (NCFP) methods were later successfully applied to study a wide range of suctions from 10 kPa to 100 MPa (Acikel et al., 2011, 2015; Hanson et al., 2013; Risken et al., 2016). In the CFP method, it was found that capillary breaks were more likely to occur while filter paper was in contact with a nonwoven geotextile than a woven geotextile (Acikel et al., 2015). Seiphoori et al. (2016) performed experiments on reconstituted GCLs using NCFP and a dew point method to investigate a range of suctions from 20 kPa to 110 MPa (under no load) and concluded that the SWCC of their GCL was entirely controlled by the bentonite at suctions higher than 2 MPa.

A number of experiments have been successfully conducted using relative humidity sensors (Beddoe et al., 2010, 2011; Abuel-Naga and Bouazza, 2010; Hanson et al., 2013) or by controlling relative humidity using vapour equilibrium techniques (VET) (Rouf et al., 2014, 2016). Rouf et al. (2014) reported that the time to reach equilibrium depends on a number of factors and it may exceed 1 month for VET. In a recent study, Abuel-naga and Bouazza (2016) showed that gravimetric water content of a GCL specimen increased from nearly 10% to only 18.6% while it was exposed to air with a high humidity of 100% in a desiccator chamber for one year. The air was circulated in the chamber through a pump. In addition, the methods based on relative humidity are considered to be reliable only for the dry end of the SWCC curve (Agus and Schanz, 2007).

SWCCs often exhibit hysteretic behaviour, and a non-unique relationship exists between soil suction and degree of saturation under cycles of wetting and drying. Beddoe et al. (2011) and Hanson et al. (2013) studied SWCCs along wetting and drying paths for different GCL types. It was found that the manufacturing method and configuration of the geotextiles can significantly affect the SWCC of GCLs and the magnitude of hysteresis between the wetting and drying curves (Beddoe et al., 2011).

It has been shown that change in void ratio, temperature, and concentration of salt can alter retention capacity of a porous media (Olivella et al., 1994). The effect of applied stress and void ratio have been widely investigated for a range of soils and it is reported that both air-entry values - the suction at which transition to unsaturated state starts along the drying path - and air-expulsion - the suction at which transition to saturated state starts along the wetting path - change with void ratio (e.g., Tarantino, 2009). Gallipoli (2012) proposed a modified version of the van Genuchten (1980) SWCC and introduced a power function for the evolution of the air-entry suction due to void ratio change. The power nature of the relationship between air-entry suction and void ratio was later confirmed mathematically and validated experimentally for fractal soils by Russell (2014). Zhou and Ng (2014) extended the model by Gallipoli (2012) to consider the effects of pore structure using a micro-structural state variable.

Currently, the effect of volume change of a GCL on the evolution of its SWCC is not well understood. Southen and Rowe (2007) performed tests with different stresses to investigate volume change along a drying path. Bannour et al. (2014) investigated the effects of load and no change in the air-expulsion suction or slope of the SWCC was observed. On the other hand, Southen and Rowe (2007) found that the air-entry suction of GCLs varied between 50 and 200 kPa depending on the applied load.

Grant and Salehzadeh (1996) developed a chemical-thermodynamic explanation for the effects of temperature on SWCC for non-deformable media – based on the model of Philip and de Vries (1957) for liquid-gas interfacial tension. They implemented a model in the van Genuchten (1980) SWCC in which the effects of temperature were assumed to be only due to a change in the surface tension of pure water. However, experiments indicate that other processes may be involved such as changes in inter-particle bond strength, particle volume and pore water volume, soil fabric, and intra-aggregate fluid chemistry (Romero et al., 2001; Gao and Shao, 2015). The model by Grant and Salehzadeh (1996) has been implemented subsequently in more comprehensive THM theories considering effects of both deformation and temperature on SWCC such as the non-isothermal model by Zhou et al. (2014) based on the original framework proposed by Sheng et al. (2008).

Despite the large number of experiments on SWCCs of GCLs, the only systematic investigation of the effects of temperature appears to have been conducted by Risken (2014) using a filter paper method. It was observed that temperature had a small effect on the air-expulsion suction of the GCL along the wetting path, with water retention of the GCL decreasing with increasing temperature. However, no effect was observed on the drying path. Risken (2014) concluded that the decrease in the retention capacity of GCL may be attributed to a reduction of water surface tension with increasing temperature. In addition, it was suggested that complications associated with filter paper calibration under conditions other than 20 °C and 0 kPa may be responsible for masking the effect of temperature on the SWCC of GCL.

The objective of this paper is to report and analyse results of SWCC measurements for GCLs with different void ratios and controlled temperatures in order to develop SWCC equations that better reflect conditions of high-temperature and low overburden stress encountered in brine ponds and other engineering applications of GCLs. This is achieved in four stages. First, modified SWCC equations are proposed. Second, a set of SWCC of GCL is measured experimentally at different applied loads and temperatures, and compared to experimental results found in the literature. Third, measured SWCCs are used to calibrate and validate the new SWCC equations. Finally, the ability of the new SWCC equations to predict experimental results for SWCCs of two types of needle-punched GCLs reported by Southen and Rowe (2007) are assessed.

3. Theory

The effects of deformation and temperature on the water retention of soils are active fields of research. Various method for the evaluation of the effect of void ratio or deformation on the degree of saturation have been recently proposed in the literature based on different theoretical conceptualization of the coupling between mechanical and hydraulic behaviour of clay (Khalili et al., 2008; Casini et al., 2012; Sheng and Zhou, 2011). However, no consensus has yet emerged about the best theoretical approach to the problem.

Gallipoli (2012) extended the van Genuchten's equation to incorporate the effect of change in void ratio on the SWCC of a deformable medium through a modification of the air-entry parameter which is expressed as a power function of void ratio. Similar approaches have been used in other SWCC equations (Tarantino, 2009; Hu et al., 2013; Russell, 2014). Grant and Salehzadeh (1996) introduced a modified version of van Genuchten's equation to consider the effect of temperature for a non-deformable medium based on the theory of Philip and de Vries (1957) which considers change in surface tension of water due to temperature.

In this section, implementation of combined theories of Grant and Salehzadeh (1996) and Gallipoli (2012) in van Genuchten (1980) SWCC is presented. In addition, the same approach is applied to the Fredlund and Xing (1994) SWCC. The van Genuchten version (VG version) can be expressed as:

$$S_r = S_{rs} + (S_s - S_{rs})\left(1 + \left(\frac{s}{P_0 \frac{\sigma}{\sigma_0}\left(\frac{e}{e_{ref}}\right)^{-\beta_e}}\right)^{\frac{1}{1-\lambda}}\right)^{-\lambda} \quad (1)$$

where:

S_r = degree of saturation of liquid phase
S_{rs} = residual degree of saturation of liquid phase
S_s = maximum degree of saturation of liquid phase
P = model parameter that is representative of air-entry value, kPa
λ = model parameter that controls slope of curve
e = void ratio
P_0 = model parameter measured at a reference void ratio of e_0, kPa
β_e = model parameter
e_{ref} = reference void ratio
σ = surface tension at current temperature, N/m
σ_0 = surface tension at reference temperature, it is 0.072 N/m at 20 °C
s is matric suction defined as:

$$s = P_g - P_l \quad (2)$$

where:

P_g = gas pressure (compression is positive), kPa
P_l = liquid pressure (compression is positive), kPa

The Fredlund and Xing version (FX version) is:

$$S_r = C(s)\left\{\ln\left[\exp(1) + \left(\frac{s}{a_{f0}\frac{\sigma}{\sigma_0}\left(\frac{e}{e_{ref}}\right)^{-\beta_e}}\right)^{n_f}\right]\right\}^{-m_f} \quad (3)$$

where the correction factor $C(s)$ is:

$$C(s) = 1 - \frac{\ln(1 + s/\psi_r)}{\ln[1 + (10^6/\psi_r)]} \quad (4)$$

where:

a_f = a parameter to be determined from air-entry value, kPa
n_f = a parameter to be determined by rate of water extraction from soil once air-entry value is exceeded
m_f = a parameter to be determined by residual water content
ψ_r = soil suction corresponding to the residual water content, kPa.
α_{f0} = model parameter at reference σ_0 and e_0, kPa

To calculate surface tension, the equation given by the International Association for the Properties of Water and Steam (IAPWS R7-97 2012) was used in this study, viz:

$$\sigma = 0.2358\left(1 - \frac{T + 273.15}{T_c + 273.15}\right)^{1.256}\left(1 - 0.625\left(1 - \frac{T + 273.15}{T_c + 273.15}\right)\right) \quad (5)$$

where: T = temperature, °C.$T_c = 373.95°C$, critical temperature.

4. Experimental program

Three different devices were used to measure a wide range of suctions: 1) pneumatic suction-controlled oedometer, 2) WP4C, and 3) Vapour Sorption Analyzer (VSA) (Table 1). Fig. 1 shows an overview of the suction range covered in this study. SWCC tests were performed for matric suctions from 0 to 700 kPa along the drying path, using pneumatic suction-controlled odometers (Barcelona Cells). In addition, WP4C and VSA were used for measurement of total suctions from 100 to 10 MPa along the wetting path and 30–250 MPa following the drying path. VSA is able to control the humidity of a specimen and enable the drying and wetting paths of SWCCs to be measured. The time required to reach equilibrium using VSA which depends on temperature, suction, and change in suction from the previous step is relatively short. Moreover, it has been shown that WP4C measurements are accurate for suctions higher than 1 MPa and the accuracy improves as suction increases (Agus and Schanz, 2007; Campbell et al., 2007). Therefore, the WP4C was used to provide confirmation of the suction measurements made by VSA.

All experiments were performed under temperature-controlled conditions. Isothermal oedometer, WP4C, and VSA experiments were conducted at temperatures of 20 and 35 °C. Additional experiments at 40 and 60 °C were performed using the oedometer and VSA, respectively. Moreover, constant net vertical stresses of 10, 20, and 50 kPa were applied to the specimens in experiments conducted using the oedometer.

In this study, matric suctions were measured for low suctions (< 700 kPa) and total suctions for high suctions (> 10 MPa). Total suction is the sum of matric suction and osmotic suction. The magnitude of osmotic suction depends on concentration of dissolved salts. Therefore, at a specific water content, total suction is higher than matric suction and the difference between matric and total suction increases as water content decreases (e.g. see Leong et al., 2003). Beddoe et al. (2011) and Rajesh and Khan (2018) reported that, for GCLs, the difference between matric and total suction at high range of suction (> 35 MPa) is negligible compared to the magnitude of suction.

In the present study, the magnitude of osmotic suction for experiments is not clear and no correction was performed to adjust the values of measured suctions.

4.1. Axis-translation: pneumatic suction-controlled oedometer (Barcelona cell)

Tests were performed using suction-controlled oedometers (Romero et al., 1995) following the guidelines from ASTM D6836 (2008) and ASTM C1699 (2009). Axis-translation is based on the principle that a desired matric suction can be applied to a soil by controlling pore-gas and pore-liquid pressure. The liquid pressure was kept constant using a liquid volume-pressure controller (GDS) and gas pressure was adjusted to reach the target matric suction. A porous ceramic disk (or a membrane) is required in axis-translation to separate the gas and liquid phases and the maximum possible suction is hence limited to the air-entry value of the porous ceramic disk. To ensure the ceramic disks were saturated, they were submerged in de-ionised and de-aired water for at least 24 h, then de-ionised and de-aired water was flushed with 700 kPa pressure through the ceramic disk for around 1 h and the flushing was repeated with freshly de-aired water until no air was observed to flow out. A kaolin paste was prepared according to ASTM C1699 (2009) by mixing 125 g of kaolin powder and 150 g distilled water. The paste with a thickness of ≈1 mm was directly applied onto the saturated ceramic disk. The kaolin paste ensured good hydraulic contact between the GCL and the ceramic disk in order to prevent capillary breakage (Southen and Rowe, 2007; Abuel-Naga and Bouazza, 2010; Beddoe et al., 2010). In addition, the specimen was rotated by 45° after installation for a better hydraulic contact. Several preliminary tests were conducted and it was observed that using the paste and rotation considerably reduced the required time to reach equilibrium under higher suctions (i.e. 350 and 700 kPa).

The specimen was placed in the oedometer after hydration and the desired suctions were applied following the drying path. To be able to obtain the air-entry value of the specimen, it is recommended that the first applied suction be below one-half the anticipated air-entry value (ASTM D6836). The oedometers were placed in the temperature-controlled environment (laboratory water bath) at the target temperature for at least 24 h before the SWCC measurements started, to make sure that the cells were in thermal equilibrium.

Table 1
Experimental program.

Test device	Test method	Net vertical stress (kPa)	Temperature (°C)	Suction	Matric/Total suction	Path
Oedometer	Axis-translation	10, 20, 50	20, 35, 40	0–700 kPa	Matric	Drying
WP4C	Dew point	0	20, 35	100 to 10 MPa	Total	Wetting
WP4C	Dew point	0	20,35	30–250 MPa	Total	Drying
VSA	Dew point	0	20, 35, 60	100 to 10 MPa	Total	Wetting
VSA	Dew point	0	20, 35, 60	30–250 MPa	Total	Drying

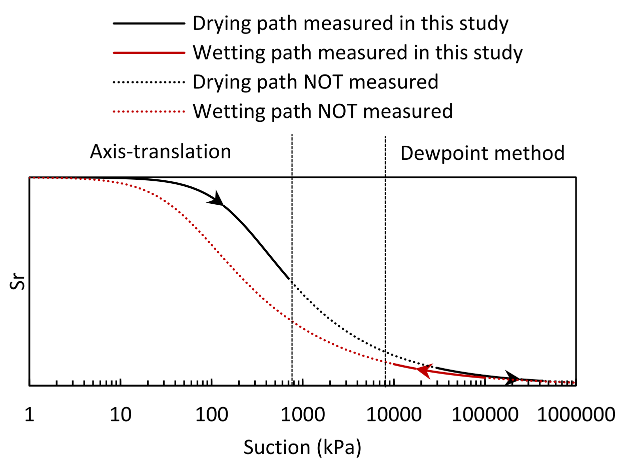

Fig. 1. Overview of methods used and suction range covered in this study.

Suctions from 0 to 700 kPa were imposed in successive stages to obtain the SWCC. At each applied suction, hydraulic equilibrium must be reached before a reading of water content is made. According to ASTM C1699 (2009), equilibrium can be considered to have been reached when water outflow is less than 50 mm^3 in 48 h. For GCLs, achieving equilibrium may take several days or weeks depending on the applied suction and temperature. Furthermore, the equilibrium state for a GCL can be confirmed based on the rate of axial strain, similar to ASTM D2435/D2435M (2011) under each matric suction step.

4.2. Dew point method: WP4C and VSA

"Dewpoint PotentiaMeter WP4C" and VSA devices are based on an accurate measurement of the partial pressure of vapour in a small sealed chamber above a specimen using the dew point of vapour under equilibrium with the specimen (Campbell et al., 2007). At equilibrium, the partial pressure of vapour in the chamber and the partial pressure of pore-water vapour of the specimen are equal. A small fan in the chamber reduces the time it takes to reach equilibrium. The air space acts as a perfect semi-permeable membrane; therefore, total suction is measured using the dew point method.

VSA provides two different methods to perform SWCC tests: 1) the dynamic vapour sorption method (DVS); and 2) the dynamic dew point isotherm method (DDI). In the DVS method, a specimen is exposed to a controlled humidity and the change in the mass of specimen is tracked until the specimen reaches equilibrium and the rate of change of mass of the specimen reduces to a limit (typically 0.02% per hour). On the other hand, the DDI method dries or wets the specimen under a constant flow of air; however, neither change in mass of specimen nor humidity is controlled; as a result, the specimen may not be at equilibrium at the time of the suction measurements. Therefore, the DVS method was considered more reliable than DDI and was used to perform the tests in this study.

For measurement of height of specimens, a setup similar to the apparatus described in ISO 9863-1 (2016) was used which significantly enhanced the accuracy of measurements (Fig. 2). After each step was completed, the heights of the specimens for all dew point method experiments were measured under a small load of 2 kPa. The load was applied by a steel block, while the specimen was confined in its cup. However, during suction measurements, it is not possible to apply a load to the specimen in the dewpoint method.

VSA and WP4C were used to measure total suctions for the dry ends of the curves. In practice, composite geosynthetic clay liners may experience temperatures as high as 95 °C in brine ponds (Rowe, 2012), although to extend the service-life of the geomembrane liner efforts are often made to control the temperature to 60 °C or below (Rowe and Shoaib, 2018). The experiments in this study were performed under temperatures of 20, 35, and 60 °C using VSA and only 20 and 35 °C for the WP4C because of limitations of the devices. Both VSA and WP4C have built-in temperature control units.

4.3. Material

The GCL used in this study (ELCOSEAL GCL grade X2000 by GEOFABRICS Australia; Table 2) had a powdered Na-bentonite layer encased between a polypropylene nonwoven and woven needle punched carrier geotextile and polypropylene nonwoven cover geotextile with the components held together by needle-punching and thermal treatment. The as-received gravimetric water content of the GCL was between 8.5 and 9.5%.

4.4. Specimen preparation

Specimens from the GCL sheets were cut at the as-received moisture content. The mass of each specimen was measured and then the specimen was sealed in double plastic zip bags and stored in an air-tight container. Dies made of steel were used to minimize bentonite loss when cutting GCL specimens. Nevertheless, the smaller size specimens had slightly lower average mass per area compared to the larger specimens, which is likely due to bentonite loss during the cutting process. Mass per unit area of bentonite can significantly affect the hydraulic properties of a GCL. Therefore, specimens with estimated mass per areas close to the typical value were selected for testing.

For SWCC tests using the axis-translation method, a setup similar to an oedometer was used to hydrate GCL specimens under specific loads. The setup allows the volume change to be measured during hydration without disturbing the specimen. It includes a confining ring with a diameter of 50 mm and a height of 20 mm made of stainless steel, two porous stones for top and bottom of specimen, a mould, a dial gauge, and a load hanger. Using a stainless-steel ring for hydration ensures that only one-dimensional deformation of the GCL occurs in the process. In addition, the ring prevents bentonite loss and maintains the circular shape of the specimen during hydration.

The confining ring containing the GCL was submerged in tap water with a total dissolved solids (TDS) of 100–136 mg/l and allowed to hydrate at room temperature (23 ± 1 °C) for more than a month under a specific load applied by the hanger. Swelling of the specimen was measured using the dial gauge and it was assumed that the specimen had reached its maximum hydration once swelling stopped. The normal stress during the hydration stage was 2 kPa for the specimens that were tested under 10 kPa in the Barcelona cell. However, for SWCC tests where specimens were subjected to net normal stresses of 20 and 50 kPa, the load during hydration was 20 kPa. It is generally not

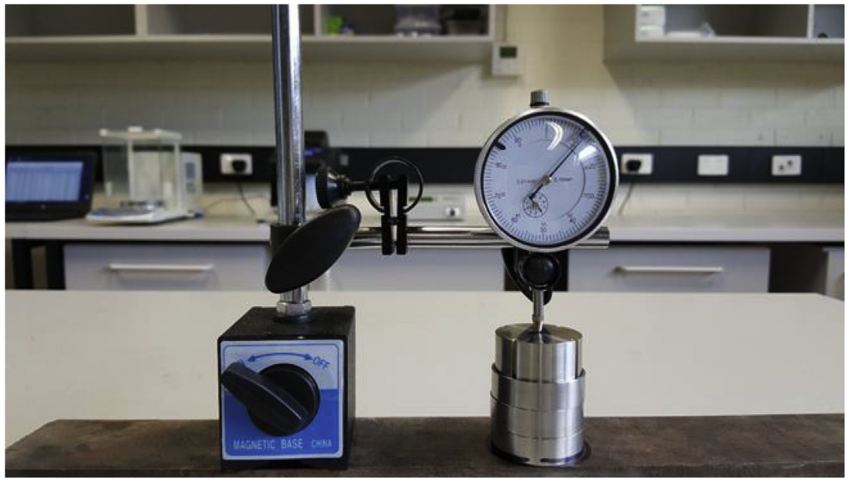

Fig. 2. GCL height measurement setup: the setup is a modification of ISO 9863-1 (2016).

possible to fully saturate GCL specimens without applying a back pressure and in this study the specimens reached a high degree of saturation (85% and above). Although full saturation was never achieved, the GCL water content, w_{ref}, represents the maximum gravimetric water content that could be encountered in a real field situation at the same stress. As is common when dealing with GCLs, in this paper S_r is taken to be the apparent degree of saturation which is the gravimetric water contents, w, divided by w_{ref} (i.e., $S_r = w/w_{ref}$).

SWCCs can be expressed using gravimetric water content, volumetric water content or degree of saturation as the dependent variable. Converting between these three variables requires knowledge of the void ratio of the specimen. However, the GCL is a composite material and the void ratios of the components can be different. Therefore, the bulk void ratio of the GCLs was used in this study (Petrov and Rowe, 1997). For each specimen, the height of solids was calculated based on the total mass per area of the specimen and it was assumed that the typical values of mass per area of geotextiles (reported by the manufacturer) were the actual values for all specimens and any difference in the mass of the GCL was due to differences in the mass per area of bentonite. This assumption complies with guidelines for measurement of mass per unit area of GCLs provided by ASTM D5993 (2009) "Standard Test Method for Measuring Mass Per Unit of Geosynthetic Clay Liners".

5. Results

5.1. Effects of load

Figs. 3 and 4 show the effect of load on the SWCC and void ratio following the drying path under 20 and 35 °C, respectively. At 20 °C, an increase in net axial stress from 10 kPa to 20 kPa decreased void ratio of the specimen for the same suctions (Fig. 3-b) and increased air-entry suction and slope of the SWCC (Fig. 3-a). This is consistent with reported effects of void ratio changes on SWCCs of porous media (e.g. see Romero et al., 2001; Gallipoli et al., 2003; Tarantino, 2009). The significant difference between void ratios of tests under 10 kPa and 20 kPa is believed to be due to the different stresses applied during hydration of the specimens. As stated earlier, the specimens for tests under 10 kPa and 20 kPa were hydrated under 2 kPa and 20 kPa overburden stresses, respectively. Therefore, it is possible that fibres were pulled out of the specimen that was hydrated under 2 kPa load as a result of swelling pressure of bentonite, which could have led to higher void ratios and higher gravimetric water contents, at saturation. For tests at 35 °C, a higher net axial stress caused lower void ratio. However, the change in the air-entry value is not significant (Fig. 4-a).

The slopes of the SWCC, λ, for the experiments under higher net stresses are slightly higher than those performed under lower stresses at the same temperature (Figs. 3-a and 4-a). This is consistent with the

Table 2
GCL properties reported by the manufacturer. Typical values are presented.

Property	Test method	Unit	GCL1
Configuration (Carrier/Cover)		–	W + NW/NW
k_s	ASTM D5887	m/s	1.6×10^{-11}
$M_{GCL\ @\ w=0\%}$	ASTM D5993	g/m^2	4960
$M_{Bentonite\ @\ w=0\%}$	ASTM D5993	g/m^2	4250
M_{cover}	AS 3706.1	g/m^2	300
$M_{carrier}$	AS 3706.1	g/m^2	410
Hydrated peak internal shear strength under 10 kPa normal stress	ASTM D6243	kPa	35
Hydrated peak internal shear strength under 30 kPa normal stress	ASTM D6243	kPa	60
Bentonite particle size	AS 1286–3.6.2	passing 75μm	≥ 75%
		passing 0.5 μm	≥ 55%
Bentonite swell index	ASTM D5890	mL/2 g	≥ 24
Montmorillonite content	XRD QM	% of bulk specimen	≥ 70
		% of particle passing 0.5μm	≥ 90
Calcium carbonate content ($CaCO_3$)	XRD QM	% of bulk specimen	≥ 2
Cation exchange capacity	NH_4 DM BSM	cmol/kg	70–110

W: Woven; NW: Non-Woven; XRD: X-ray diffraction; QM: Quantitative mineralogy analysis; DM: displacement method; BSM: Barium saturation method; The typical values are the arithmetic mean of the measured values. As provided by the manufacturer.

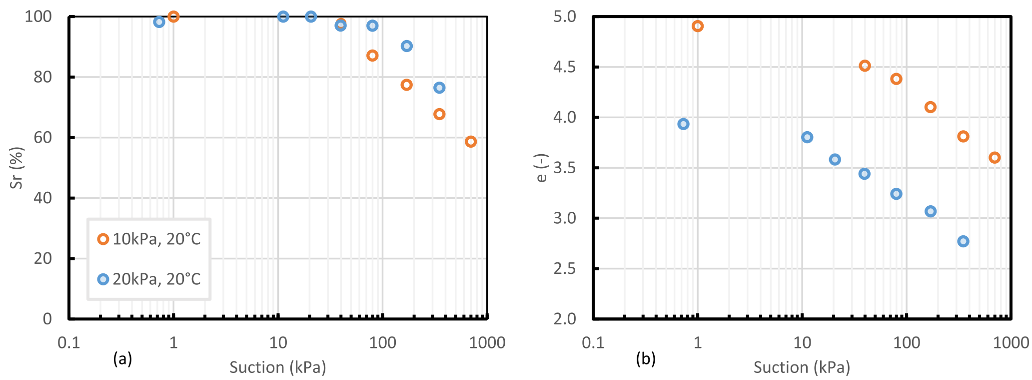

Fig. 3. Effect of load on SWCC at 20 °C: Degree of saturation vs suction; b) Void ratio vs suction.

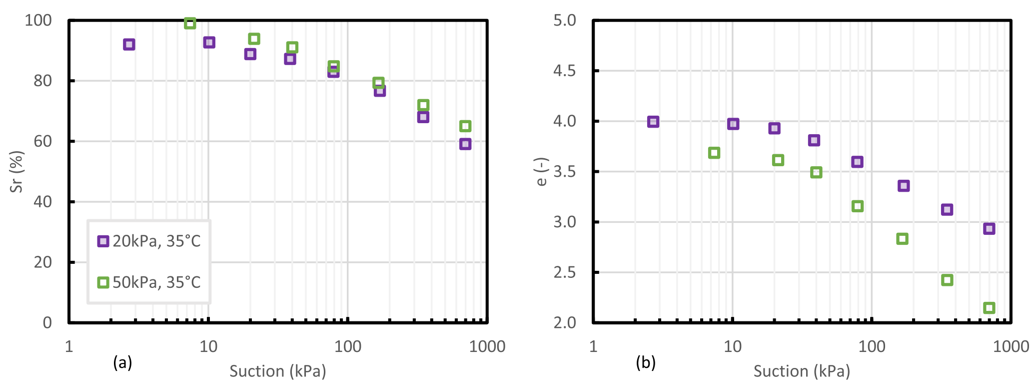

Fig. 4. Effect of load on SWCC at 35 °C: Degree of saturation vs suction; b) Void ratio vs suction.

effect of void ratio on slope of SWCC of white clay (Khalili et al., 2008). However, data points at higher suctions are required to be able to clearly characterize the effect of void ratio on the slope of the SWCC of GCLs.

In Fig. 3-b, κ_s, the slope of $e - \ln(s)$, is essentially the same for the tests under 10 and 20 kPa. On the other hand, the slope of the curve for test under 50 kPa is higher than that of 20 kPa (Fig. 4-b). This is not consistent with the effect of load on other porous materials which have shown that a higher net stress can result in a lower slope of SWCC for clay and clayey sand (Lloret and Alonso, 1980, 1985).

Fig. 5-a, b, and c show X-ray images of three specimens at nearly saturated (w = 180%), a matric suction of 170 kPa (w = 135%), and a matric suction of 350 kPa (w = 100%), respectively. Despite retaining a relatively high gravimetric water content of 100%, the specimen under the matric suction of 350 kPa (Fig. 5-c) experienced significant cracking and shrinkage. Moreover, cracks were observed at the suction of 170 kPa (Fig. 5-b); while, there was no sign of cracking in the specimen at nearly fully saturated condition (Fig. 5-a). It is essential to further investigate the effects of the cracks on the hydraulic performance of GCLs.

5.2. Effects of temperature

To evaluate the effects of elevated temperatures on the SWCC along drying paths, two main factors should be considered (Zhou et al., 2014): 1) reduction of surface tension of water; and, 2) softening of the soil. The former factor results in a lower retention capacity in terms of both degree of saturation and gravimetric water content because a lower surface tension of water reduces capillary pressure and the capacity of the soil to hold water (Grant and Salehzadeh, 1996). However, softening can result in a lower void ratio (Campanella and Mitchell, 1968) which can lead to two counter-acting processes: 1) increasing capillary pressure because of smaller pore sizes (Khalili et al., 2008; Gallipoli, 2012); 2) squeezing water out and reducing the total amount of water. In addition, other factors such as changes in pore water chemistry and the different thermal expansion of different phases can influence the resulting SWCC (Romero et al., 2001).

Fig. 6 presents the effects of temperature on the retention capacity

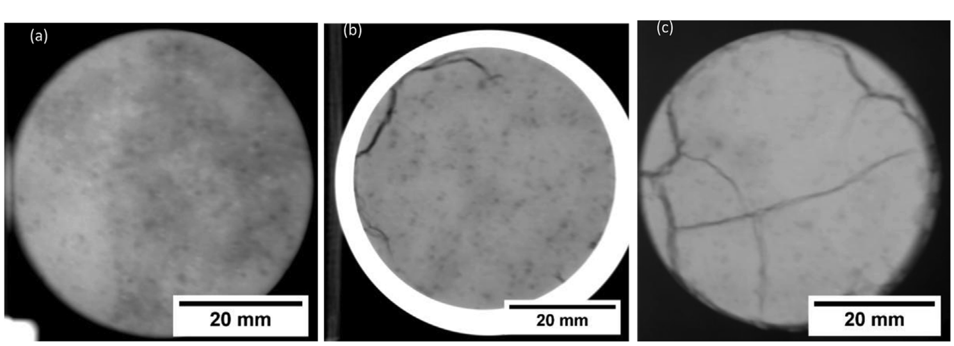

Fig. 5. X-ray image of GCL specimens at: a) nearly fully saturation; b) a matric suction of 170 kPa; c) a matric suction of 350 kPa.

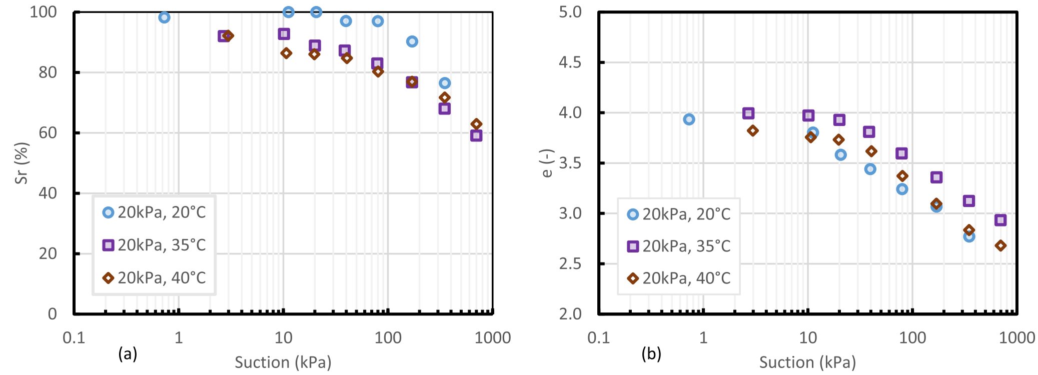

Fig. 6. Effect of temperature on SWCC under net axial stress of 20 kPa (axis-translation method): Degree of saturation vs suction; b) Gravimetric water content vs suction.

of the GCL in terms of degree of saturation and gravimetric water content under a net axial stress of 20 kPa using axis-translation. The experiments indicate that a higher temperature produces a lower retention capacity for the same net vertical stress (Fig. 6) in terms of both gravimetric water content and degree of saturation. A major limitation in the axis-translation method experiments is that a relatively long time is required to reach equilibrium for each point at higher suctions. The length of each experiment to obtain the curves was more than 2 months in this study.

Fig. 7-a shows that for the high suction range, the differences in degrees of saturation with temperature are not significant nor is there any trend for experiments performed at temperatures between 20 and 60 °C for drying path using the dewpoint method. In addition, temperature seems to have no effect on the retention capacity of the GCL in terms of gravimetric water content (Fig. 7-b). Therefore, evidence gathered here does not support the view that the SWCC is temperature dependent on the dry end of the curves.

5.3. Hysteresis

As described before, SWCC tests on both drying and wetting paths were performed on the dry side of the curve (i.e. suctions higher than 10 MPa) using the dewpoint method. However, only the drying path was studied on the wet side of the curve (i.e. suctions lower than 700 kPa) because of difficulties associated with GCL SWCC tests using axis-translation method.

For the dewpoint method, the starting point of the test was the as-received water content and suction of the specimen. The starting point was measured using the WP4C (the blue triangles on Fig. 8) for experiments under 20 and 35 °C. Then the VSA was used to follow a wetting path using controlled relative humidity in two steps to an ultimate suction of ≈10 MPa. Next, the drying path was followed in three steps to a suction of nearly 250 MPa. The upper and lower limits for suctions were selected based on the accuracy and capacity of the VSA. In each step of SWCC testing, the suction measurements from the VSA were cross checked with the WP4C. For the experiments performed at 60 °C, only the VSA was used, following the protocol described above.

Comparisons of the VSA and WP4C measurements under temperatures of 20 and 35 °C are presented in Fig. 8, and show similar responses. There is evidence of some slight hysteresis in the experiments with the drying path showing slightly higher degrees of saturation. Void ratios show a relatively consistent trend, increasing as suction decreases and vice versa (Fig. 9). However, a small hysteresis is observed in the void ratio changes and void ratios on the drying path are slightly higher than those on the wetting path, except for one reading for test under 35 °C at suction of 260 MPa, which may be a measurement error.

The time required to reach equilibrium is relatively short for the VSA and depends on the applied suction, the amount of change in suction from the previous step, and temperature. It was observed that the rate of change in water content and suction depends on the temperature and experiments under higher temperature reached equilibrium faster. In this study, the time to reach equilibrium for each point was less than a week.

5.4. Comparison to existing GCL SWCCs

This section presents a comparison between the SWCCs of GCL1 (under 20 and 35 °C) and two sets of SWCCs found in the literature, performed at room temperature. The two sets are the experiments by a) Southen and Rowe (2007) on two types of GCLs, one granular (SR07G1) and one powdered Na-bentonite (SR07G2), under different loads following the drying path, and b) Abuel-Naga and Bouazza (2010) on a powdered Na-bentonite (AB10) under 50 kPa at 25 °C following the wetting path (Fig. 10-a). The void ratio, total suction relationship is also illustrated for the bentonite under free swelling condition in Fig. 10-b. A summary of the specifications of the GCLs used in these experiments is presented in Table 3.

The mass per unit area of bentonite of SR07G1 is close to the GCL

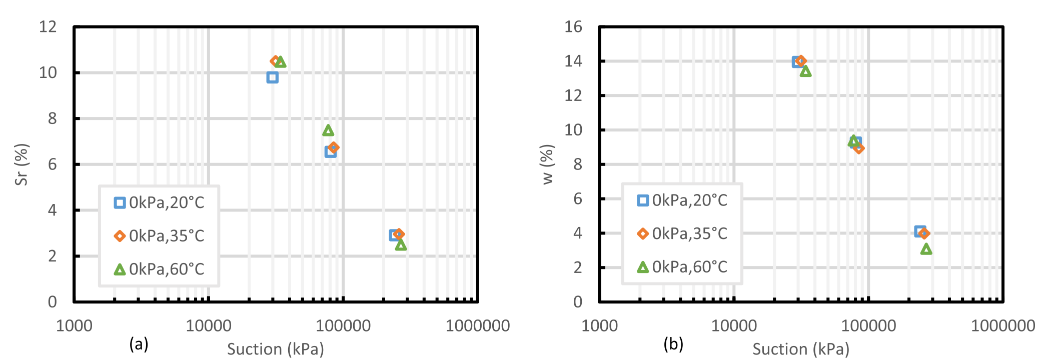

Fig. 7. Effect of temperature on SWCC under net axial stress of 0 kPa (dewpoint method): Degree of saturation vs suction; b) Gravimetric water content vs suction.

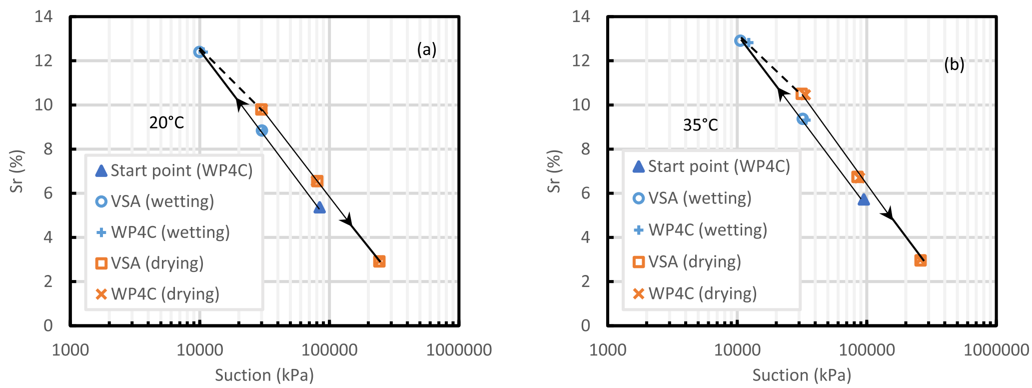

Fig. 8. Comparison of VSA and WP4C: a) 20 °C; b) 35 °C.

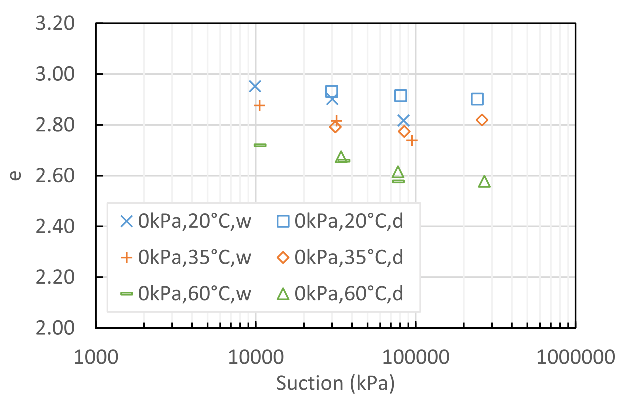

Fig. 9. Void ratio vs suction for all dewpoint method experiments. w: wetting path; d: drying path.

used in this study. The masses of bentonite per unit area of SR07G2 and AB10 are considerably higher than GCL1.

Overall, the current experimental results are similar to previously published SWCCs of GCLs (Fig. 10-a) considering the range of products and different stress levels used. Moreover, the measurements performed in this study are more consistent and less scattered than those collected from the literature. In addition, individual tests show a consistent pattern of change in void ratio. Fig. 10-b shows that void ratio of GCL is controlled by the applied vertical stress and a higher load can result in a lower void ratio. However, other factors such as mass per unit area of bentonite can affect the trend. The data on the effect of temperature on void ratio is very limited and does not show a significant effect. However, for all specimens (except SR07 3 kPa), a similar trend for change in void ratio with change in suction was observed and all specimens showed relatively large void ratio changes for a range of suctions between 10 and 10000 kPa, while change in void ratio for higher suctions became insignificant.

However, despite the care given to obtaining reliable bulk void ratios for the GCL specimens, the results will be influenced by cracking and lateral shrinkage of the specimens. X-ray images, discussed earlier, show significant cracking and thus volume changes based solely on vertical deformation will not correctly estimate the void ratio change.

In the following sections, application of the void ratio and temperature-dependent SWCCs to the experimental data generated in this study. as well as data taken from the literature is examined.

5.5. SWCC equations for GCL with effects of void ratio and temperature

Ideally, the effect of void ratio should be quantified by conducting SWCC measurements with void ratio held constant, and repeated at different void ratios with constant temperature. Because of the swelling/shrinkage of the GCL's bentonite that accompanies hydration/dehydration during SWCC measurements, it is difficult to perform constant volume SWCCs for GCLs, especially on the wet side of the curve. Recently, Lu et al. (2017) described a relatively simple constant void ratio SWCC test method for a GCL using WP4C and reported results for a wide range of suction (300 to 1 MPa) along the wetting path.

In this study, the SWCC described by equation (1) was calibrated to the experimental data in the S_r-s space, by selecting one set of data, called the reference data set (RDS), under a specific load, temperature T_{ref}, and wetting or drying path as the reference curve (i.e., the conventional form of van Genuchten SWCC). Although, in general, it would be possible to establish a reference curve based on minimum error for a reference temperature for all available data at that temperature and under different loads. The calibration followed four steps:

1. Establish the reference curve, by taking $\sigma = \sigma_0$ and $\beta_e = 0$ in equation (1) and backfitting P_0, λ, S_s, and S_{rs} to the RDS based on minimizing error in degree of saturation prediction;
2. Graphically, determine the air-entry value of the reference curve defined in step 1, as the suction at which a line tangent to the inflection point of the curve crosses the horizontal unit saturation line (see Fig. 11 for an example).
3. Define the reference void ratio e_{ref} as the value at the air-entry suction found in step 2.
4. Backfit β_e and λ to all available data points at T_{ref}, based on least squares of the error in degree of saturation prediction, and using P_0, S_s, and S_{rs} calculated in step 1.

Only points on the drying curves were used in the fitting exercises due to lack of data for low suctions on the wetting path. Moreover, no calibration was conducted for the temperature effects for two reasons. First, in this study, the theory by Grant and Salehzadeh (1996) was followed, which assumes that temperature effects can be predicted from changes in surface tension, without the need for calibration. Second, the available experimental data for the effect of temperature on the SWCC of GCL was insufficient for sensible calibration.

In principle, any set of parameters (load, temperature and path) can be used to establish the reference curve. Using different reference curves would result in different P_0 and e_{ref} which may lead to different solutions for β_e and λ. In this paper, an RDS based on a temperature of 20 °C and loads of 0 and 10 kPa was used in determining the reference curve, because this particular dataset contained the largest number of data points and covered almost the full range of suctions along the drying path. A good fit ($R^2 = 0.9959$), based on the least-squares method, was obtained for values of $P = 168kPa$, $\lambda = 0.296$, and $S_{rs} = 0$ (Table 4).

An air-entry value of $s_{ea} = 67kPa$ and $e_{ref} = 4.46$ were estimated following steps 2 and 3 (Fig. 11-a and b). Fig. 11-b shows that three distinct slopes for e versus s were found, based on the RDS, over the full range of suctions. This is consistent with behaviour of other soils such

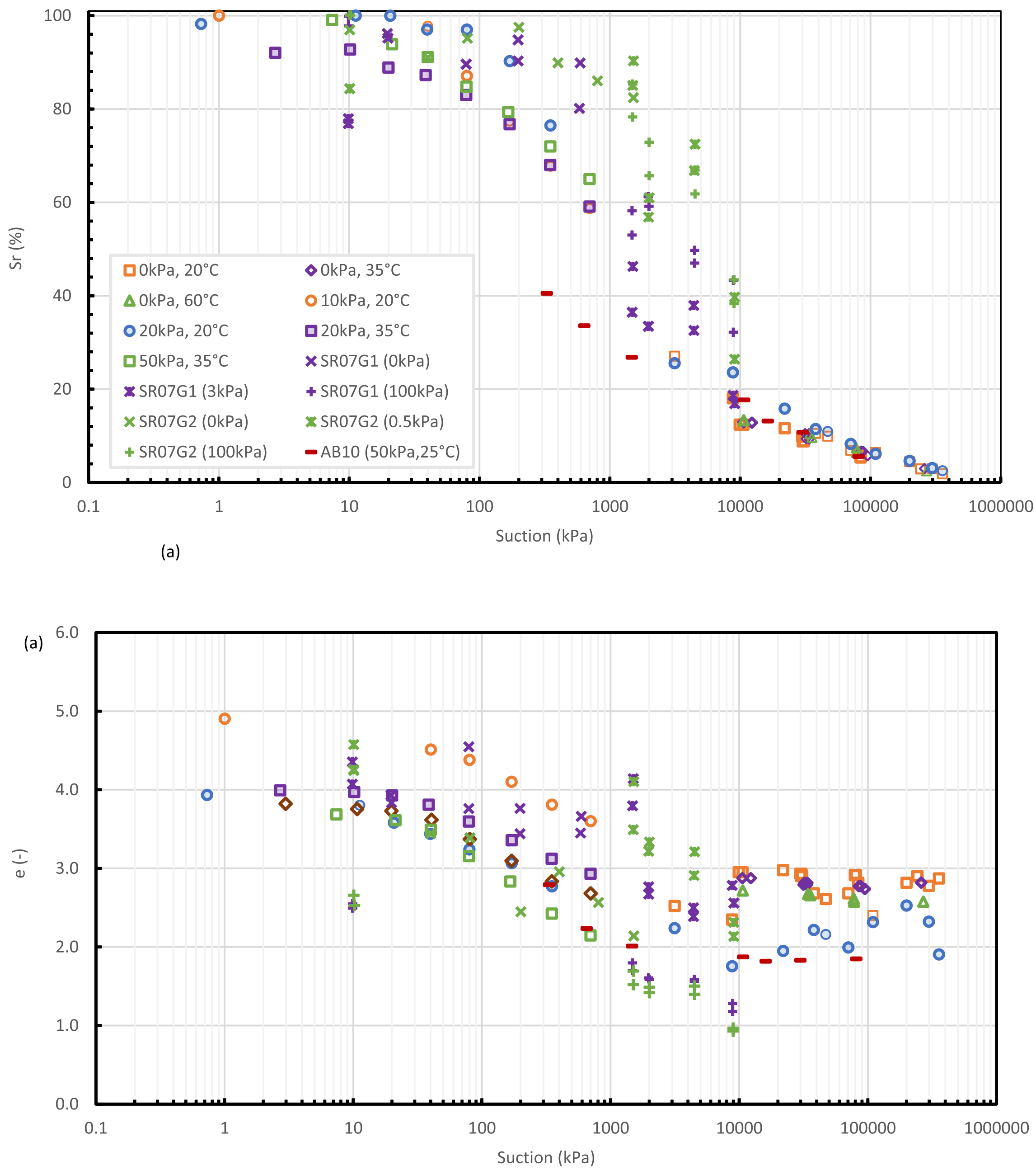

Fig. 10. SWCC tests on the GCL used in this study and comparison with SWCC of GCLs from literature. a) Degree of saturation vs. suction; b) Void ratio vs. suction. SR07: Southen and Rowe (2007); AB10: Abuel-Naga and Bouazza (2010).

Table 3
Comparison of GCL properties.

Experiment	This study GCL1	SR07G1	SR07G2	AB10
Bentonite type	PB-Na	GB-Na	PB-Na	PB-Na
Bonding	NPTT	NPTT	NPTT	NPTT
Cover geotextile	NW	NW	NW	NW
Carrier geotextile	NW + W	W	W	W
$M_{GCL}(g/m^2)$	4960	4650	5500 + 800	5500
$M_{bentonite}$ (g/m^2)	4250	4340	5000 + 800	5000
M_{cover}	300	200	300	?
$M_{carrier}$	410	105	200	?

SR07G1: Southen and Rowe (2007) on G1; SR07G2: Southen and Rowe (2007) on G2; AB10: Abuel-Naga and Bouazza (2010); PB-Na: Powder sodium bentonite; GB-Na: Granular sodium bentonite; NPTT: Needle punched thermally treated; NP: Needle punched; NW: Non-woven; W: Woven.

as white clay (Khalili et al., 2008).

In step 4, the least-squares method was used to calibrate the values of β_e and λ for the SWCC Eq. (1) based on *all* experiments at 20 °C. λ was allowed to change from its value obtained in step 1, in order to provide more flexibility in the fitting exercise. Table 4 presents the fitting parameters for the VG version of the SWCC and Fig. 12 shows predictions for the experiments under 20 °C along the drying path. A good fit was achieved with a high coefficient of determination of 0.9978 for these experiments and the maximum discrepancy between experimental and predicted values is around 4.51%. Calibration of the model based on the available data suggests $\lambda = 0.333$ and $\beta_e = 1.46$. The other parameters were obtained from the reference curve. Therefore, $P_0 = 168\ kPa$, $e_{ref} = 4.46$, $\sigma_0 = 0.0727\ N/m$, $S_s = 1.0$, and $S_{rs} = 0.0$. Note that λ obtained for the proposed SWCC is about 12% higher than that obtained for the conventional VG equation (step 1). This is due to the fact that more points were fitted to the proposed equation and some

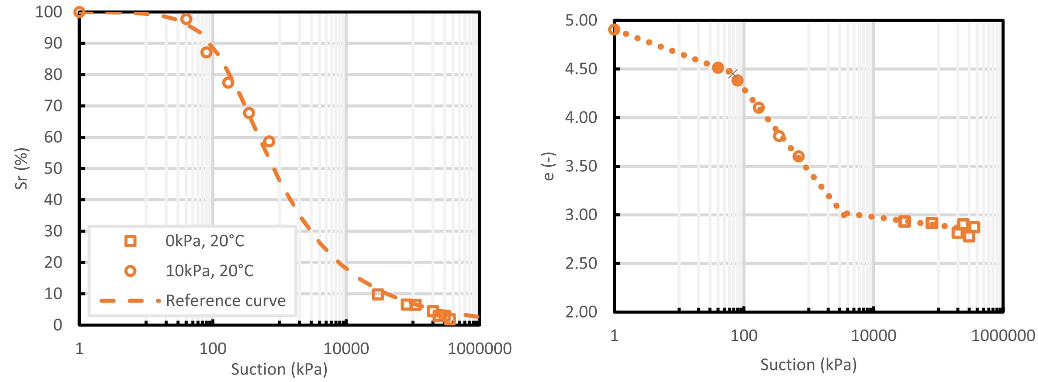

Fig. 11. Van Genuchten (1980) SWCC fit for reference curve on the drying path: a) Degree of saturation vs. suction; b) void ratio vs. suction.

Table 4
Fitting parameters for the VG version of the SWCC (Eq. (1)).

Curve	P_0(kPa)	λ	β_e	e_{ref}	σ_0(N/m)	S_s	S_{rs}
Reference curve	168	0.296	–	–	–	1.0	0.0
VG version	168	0.333	1.46	4.46	0.0727	1.0	0.0

dependence of lambda on the range of void ratios considered would be expected. Moreover, the prediction of the RDS by the void ratio dependent VG model corresponding to $\lambda = 0.333$ showed a small improvement because void ratio was considered (R^2 = 9971).

Finally, the calibrated model for all data under 20 °C was used to predict degrees of saturation at higher temperatures. Predictions were found to have an $R^2 = 0.9354$, overall. Fig. 13 shows that the proposed model performs well on the dry side of the curves; however, the predictions for low suction range are poor.

Similar steps were followed for the determination of the parameters for FX version of the SWCC (equation (3)). In step 1, the reference curve was established based on the same RDS used for the van Genuchten model. The fitting parameters obtained for the reference curve are presented in Table 5. A reference air-entry of $s_{ae} = 62kPa$ and a reference void ratio $e_{ref} = 4.46$ were estimated, which are very close to their values established for the van Genuchten equation. In step 4, the least-squares method was used to calibrate β_e, n_f, and m_f for all experiments under 20 °C. Table 5 presents the fitting parameter for the FX version of the SWCC (Eq. (3)) ($R^2 = 0.9978$). Predictions of the model for the experiments under elevated temperature conditions were slightly better for FX version ($R^2 = 0.9464$) than those of the VG version ($R^2 = 0.9354$).

As mentioned earlier, experimental measurements of SWCC should ideally be performed at a constant void ratio. However, it is not possible to maintain a constant void ratio when measuring SWCC of GCLs, because of the large volume change experienced by bentonite as suction changes. In this study, the void ratio at the air-entry value is selected for the reference void ratio. In general, selection of the reference void ratio depends on the calibration procedure. For example, considering $e_{ref} = 1.0$ would change equations 1 and 3 to a simpler form. However, for GCLs, such a void ratio at air entry suction requires a very large applied load and tends to yield a very large air-entry parameter, i.e. P_0 and a_{f0}, which may not be easily comparable with the air-entry parameters available in this study or found in the literature.

Fig. 14 shows the behaviour of the proposed SWCC indicating the effect of temperature on the proposed VG version of the SWCC for a constant void ratio and also the effect of void ratio for a given temperature. The air-entry suction decreases as void ratio or temperature increases. On the other hand, the slope of the SWCC remains the same. In this study, void ratio was allowed to change and a similar trend to

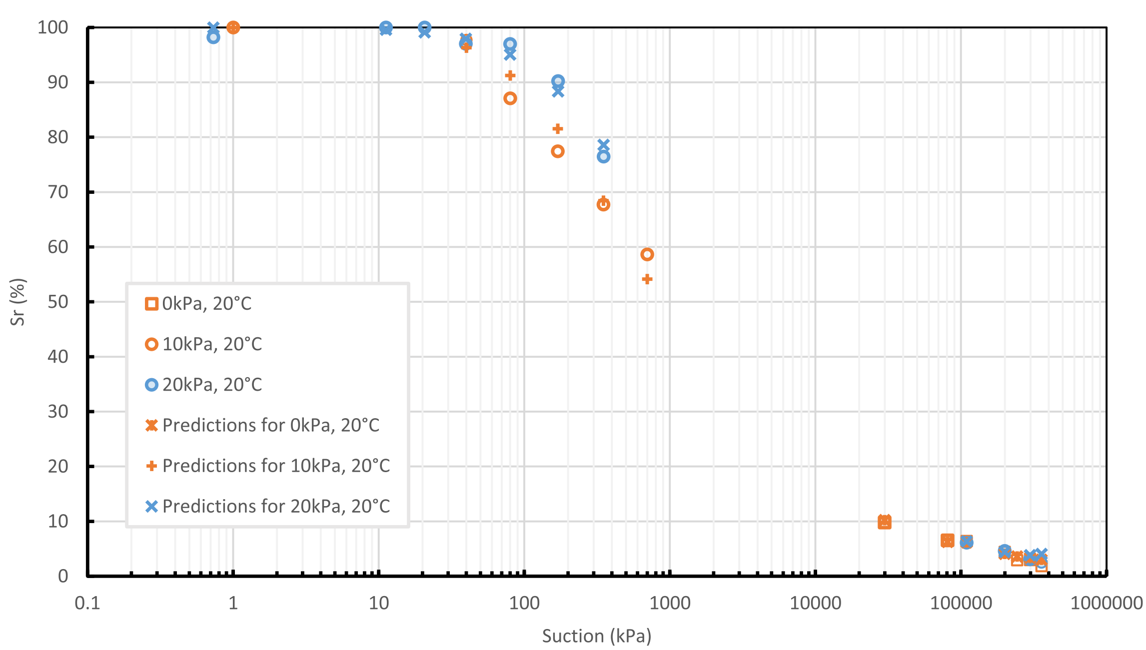

Fig. 12. Predictions for experiments at 20 °C ($R^2 = 0.9982$).

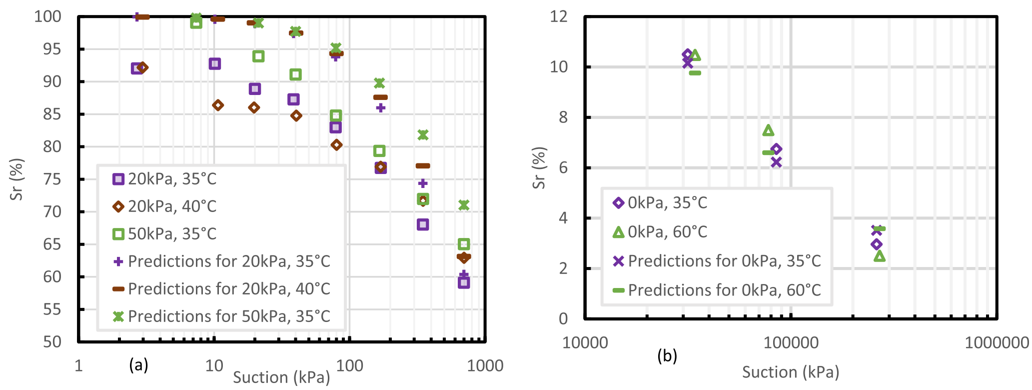

Fig. 13. Predictions based on VG version for experiments under elevated temperature conditions (R^2 = 0.9354): a) low suction range; b) high suction range.

Table 5
Fitting parameters for the FX version of the SWCC (Eq. (3)).

Curve	a_{f0}(kPa)	n_f	m_f	β_e	e_{ref}	σ_0(N/m)	ψ_r(kPa)
Reference curve	277	0.90	1.10	–	–	–	2100
FX version	277	1.06	1.20	1.60	4.46	0.0727	2100

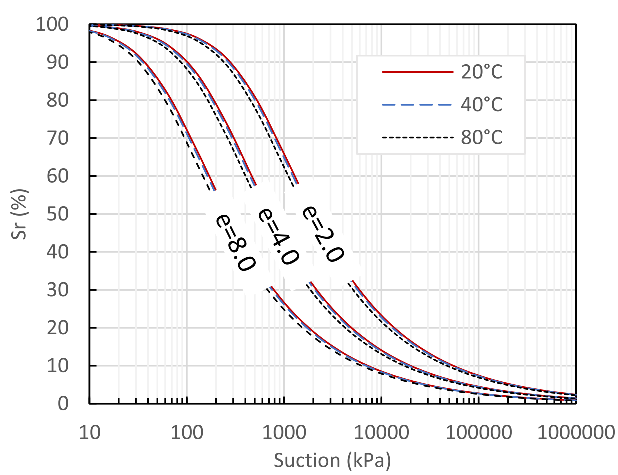

Fig. 14. The effects of temperature and void ratio on SWCC (VG version).

Fig. 14 was observed for the experiments under different net vertical stresses. The effect of temperature is more complex because Fig. 14 indicates that temperature has a relatively small effect on the retention capacity due to changes in surface tension but these predictions are not consistent with the observed behaviour of the GCL. As discussed before, other factors such as thermal consolidation and changes in pore water chemistry are believed to be more significant.

5.6. Application to existing GCL SWCC measurements

In this section, the ability of the proposed VG and FX equations to simulate the experiments reported by Southen and Rowe (2007) for two types of GCLs is examined. Specification of the GCLs have been presented in Table 3. All tests were conducted following the drying path at room temperature.

For the selection of parameters for the VG version of the SWCC (Eq. (1)), two reference curves for SR07G1 and SR07G2, were first fitted using the least-squares method, as described in step 1 earlier. However, the reference curves in this case were fitted to *all* available data for each GCL. This is because the number of data points under each combination of temperature and applied load was too small for reliable parameter fitting. In addition, the data points were scattered for both G1 and G2 experiments. The coefficients of determination for G1 and G2 were

Table 6
Fitting parameters for VG version of the SWCC (Eq. (1)).

Curve	P_0(kPa)	λ	β_e	e_{ref}	σ_0(N/m)	S_s	S_{rs}
G1-Reference curve	363	0.285	–	–	–	1.0	0.0
G2-Reference curve	1414	0.309	–	–	–	1.0	0.0
G1- VG version	363	0.324	1.0	3.20	0.0727	1.0	0.0
G2- VG version	1414	0.309	0.0	2.58	0.0727	1.0	0.0

0.7906 and 0.8009, respectively. P_0 and λ for the two respective reference curves are shown in Table 6.

Next, air-entry values of the reference curves and their corresponding void ratios at air-entry suction, e_{ref}, were estimated. The coefficients of determination of the fitted curves are low, especially for the void ratio versus suction curves. Finally, the least-squares method was used to calibrate β_e and λ based on the established values of P_0 and e_{ref} in the previous steps. Fig. 15 shows the calibrated SWCCs.

Following the procedure described above, values of P_0, λ, e_{ref}, and β_e are 363 kPa, 0.324, 3.20, and 1.002 for SR07G1 and the parameters for SR07G2 are 1414, 0.309, 2.58, and 0, respectively (Table 6). The best fit value of β_e for SR07G2 is 0. This indicates that no correlation is found between deformation and change in SWCC. On the other hand, volume change shows a significant effect on SWCC of SR07G1 and the coefficient of determination for G1 improved from 0.7906 to 0.8624. The tests were performed at room temperature which has been assumed to be 20 °C and a corresponding reference tension surface of 0.0727 N m^{-1} was adopted.

For the FX version of SWCC, using the least-squares method for the determination of a_{f0} led to an unreasonable fit which was a consequence of the data scatter (Fig. 16). Therefore, a trial and error approach was used to obtain the fitting parameters shown in Table 7. No correlation was found between degree of saturation and void ratio for G2 since β_e is 0 (Table 7), which is the same conclusion drawn earlier from the fitting exercise for G2 using VG version of the proposed SWCC.

6. Limitations

The dependence of the soil water characteristic curves of GCLs on temperature and void ratio is difficult to establish because of the highly time-consuming nature of the measurements, the complexity of the experimental procedure and the presence of hysteresis in the curves. The aim of the curve-fitting exercise in this study was to provide the best possible equation representing the SWCC, based on available experimental data, while accounting for the effects of void ratio and temperature.

Five limitations of the SWCC curves obtained here must be kept in mind. First, a full characterisation of the dependence of degree of saturation on suction, void ratio and temperature requires a larger number of experimental points than those developed here. Second,

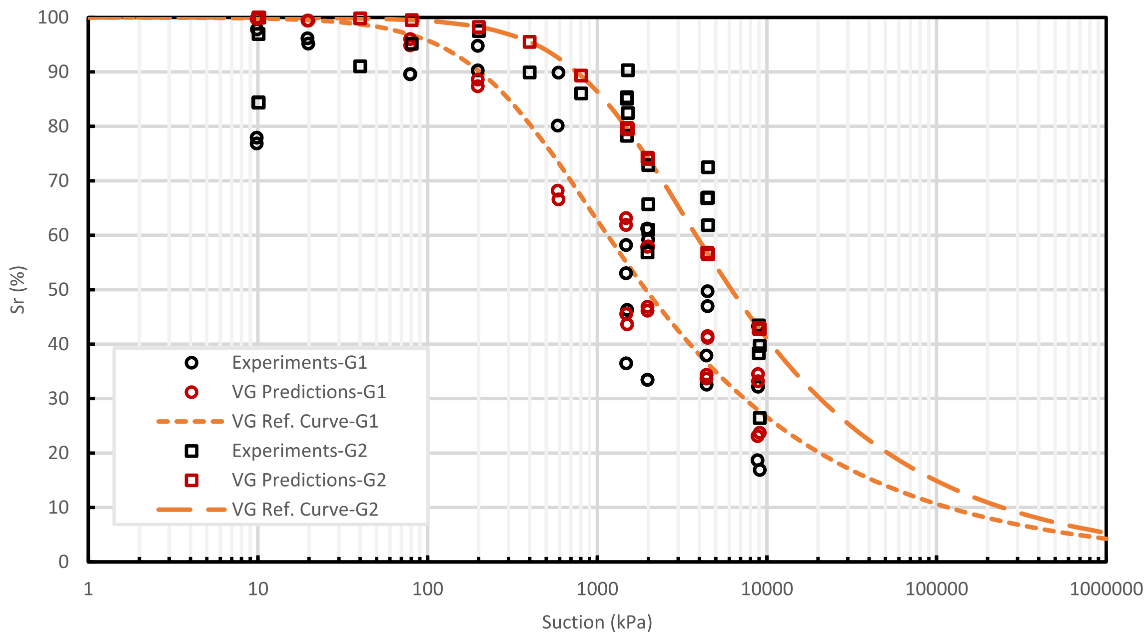

Fig. 15. VG version of the SWCC for G1 (R^2 = 0.8624) and G2 (R^2 = 0.8009).

hysteresis has been neglected in this work, and although measurements along the wetting and drying paths have been made separately, there were not enough points to develop two separate drying and wetting equations, even less to follow the hysteresis along cycles of wetting and drying. Third, the calculated degrees of saturation in this study were based on the bulk void ratio of GCL. However, X-ray images taken from specimens under different suctions revealed considerable cracking may occur on drying. Therefore, it is important to further investigate the effect of cracks on the behaviour of GCLs during SWCC tests and provide a better estimate of void ratio. Fourth, the SWCC experiments were performed under a limited range of temperature-controlled conditions. In this study, maximum temperature was limited to 40 and 60 °C for the wet (suctions lower than 700 kPa) and dry (suctions higher than 10 MPa) sides of the curves, respectively. Fifth, the effects of osmotic suction on the total suction potential and water content relationship have not been studied (matric and total suctions were measured for the wet and dry sides of the curves, respectively). Finally, the predictive approach followed here to capture the effect of void ratio is entirely statistical, based on curve-fitting. It does not start from a theoretical foundation characterising the relationship between suction, water content and void ratio. Although there is no consensus on such theory

Table 7
Fitting parameters for the FX version of the SWCC (Eq. (3)).

Curve	a_{f0}(kPa)	n_f	m_f	β_e	e_{ref}	σ_0(N/m)	ψ_r(kPa)
G1-Reference curve	360	2.32	0.45	–	–	–	2100
G2-Reference curve	1600	1.23	0.59	–	–	–	2100
G1 - FX version	360	1.65	0.65	1.17	3.18	0.0727	2100
G2 - FX version	1600	1.23	0.59	0	2.58	0.0727	2100

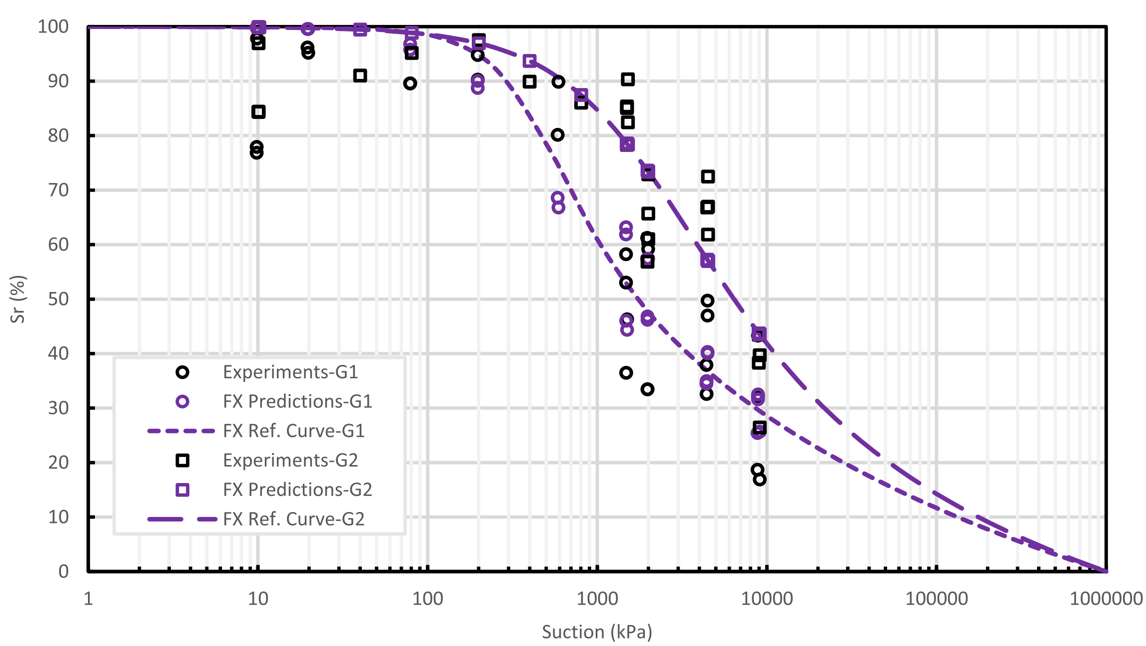

Fig. 16. FX version of the SWCC for G1 (R^2 = 0.8565) and G2 (R^2 = 0.8039).

in the literature on partially-saturated soils, there is a rich literature in this area that can inform work on SWCCs of GCLs in the future (e.g., Khalili et al., 2008; Casini et al., 2012; Sheng and Zhou, 2011).

7. Conclusions

Geosynthetic clay liners are powerful engineering materials, versatile and easy to use, which makes them cost-effective in providing hydraulic and chemical insulation in a range of engineering applications. Given the relatively short period over which experience with GCLs has accrued (just over two decades), their adequacy in applications under high temperature and low overburden load remains an open question. The aim of this study has been to characterise the dependence of the GCL's SWCC on temperature and overburden load and develop new forms of the SWCC to account for this dependence. Two new SWCCs were developed based on classical van Genuchten (1980) and Fredlund and Xing (1994), by combining theories of Grant and Salehzadeh (1996) and Gallipoli (2012).

The proposed equations performed well in predicting the effects of void ratio on SWCC based on available data. It was found that the air-entry value increases as the net vertical stress increases under the same temperature. Incorporating the effect of void ratio led to an improvement in fitting SWCC data to analytical curves for the GCL used in this study. In addition, a similar improvement was observed in analysing SWCC data for one GCL (G1) tested by Southen and Rowe (2007) but not for another one (G2).

The SWCCs underestimated the effects of elevation of temperature for the wet side of the curves. Therefore, it seems that the model based on change of surface tension with temperature is not sufficient for predicting the effect of temperature on SWCC, other mechanisms may be involved and this requires further investigation. On the other hand, modified versions of van Genuchten (1980) and Fredlund and Xing (1994) appear to have equal capabilities in representing experimentally determined SWCCs and their changes with void ratio and temperature.

Different methods were used for the SWCC measurements to cover the full range of suctions because the composite nature of GCL significantly limits the applicability of the available methods. One important issue was the possibility of a capillary break at the interface between the geotextile and the ceramic disk in the axis-translation method. In addition, SWCCs were measured mostly for the drying path because of difficulties associated with SWCC measurements under the wetting path, especially for the wet side of the curve with suctions lower than 3 MPa.

Given the above limitations, a number of future research pathways can be pursued. Despite efforts in this study and work by other authors, our understanding of the effects of temperature on SWCC of GCLs remains limited. Performing additional temperature-controlled experiments, especially on the wet side of the curves, is required to improve the developed SWCC models and the accuracy of the fitting exercise. Second, conducting similar experiments to those conducted here on different types of GCLs is necessary to characterize the effects of GCL type and manufacturing process on its performance and safety in applications with high temperature gradients. This is important because different GCL types and manufacturing processes have significant effect on hydration of GCL from subsoil and water retention capacity of GCL which are important factors in the response of a composite lining system to applied thermal gradients.

Acknowledgments

This project is funded by Australian Research Council (ARC) Discovery grant DP130100203. We are grateful to Professors David Toll and Malek Bouazza for their generous advice, Dr Mohammad Asgar Ali and Dr Md. Abdur Rouf for their help and data sharing.

References

Abuel-Naga, H., Bouazza, A., 2010. A novel laboratory technique to determine the water retention curve of geosynthetic clay liners. Geosynth. Int. 17 (5), 313–322.
Abuel-naga, H.M., Bouazza, A., 2016. Geotextiles and Geomembranes Electrical resistance method for assessing spatial variation of water content in geosynthetics clay liners at laboratory scale. Geotext. Geomembranes 44 (1), 117–121.
Acikel, A.S., Singh, R.M., Bouazza, A., Gates, W.P., Rowe, R.K., 2011. Water retention behaviour of unsaturated geosynthetic clay liners. In: 13th International Conference of the International Association for Computer Methods and Advances in Geomechanics, IACMAG 2011, vol. 2. pp. 626–630.
Acikel, A.S., Singh, R.M., Bouazza, A., Gates, W.P., Rowe, R.K., 2015. Applicability and accuracy of the initially dry and initially wet contact filter paper tests for matric suction measurement of geosynthetic clay liners. Geotechnique 65 (9), 780–787.
Agus, S.S., Schanz, T., 2007. Errors in total suction measurements. In: Experimental Unsaturated Soil Mechanics, vol. 112. pp. 59–70.
ASTM C1699 - 09, 2009. Standard Test Method for Moisture Retention Curves of Porous Building Materials Using Pressure Plates. ASTM International ASTM Standard Guide.
ASTM D2435/D2435M -11, 2011. Standard Test Methods for One-dimensional Consolidation Properties of Soils Using Incremental Loading. ASTM International ASTM Standard Guide.
ASTM D5993, 2009. Standard test method for measuring mass per unit of geosynthetic clay liners. 99. Annual Book of ASTM Standards, pp. 1–4 Reapproved 2009.
ASTM D6836, 2008. Standard Test Methods for Determination of the Soil Water Characteristic Curve for Desorption Using a Hanging Column, Pressure Extractor, Chilled Mirror Hygrometer, and/or Centrifuge. ASTM International.
Bannour, H., Stoltz, G., Delage, P., Touze-Foltz, N., 2014. Effect of stress on water retention of needlepunched geosynthetic clay liners. Geotext. Geomembranes 42 (6), 629–640.
Barroso, M.P., Touze-Foltz, N., 2006. Validation of the use of filter paper suction measurements for the determination of GCLs water retention curves. In: Kuwano, J., Koseki, J. (Eds.), 8th International Conference on Geosynthetics (8ICG), pp. 171–174 Yokohama, Japan.
Beddoe, R.A., Rowe, R.K., Take, W.A., 2010. Development of suction measurement techniques to quantify the water retention behaviour of GCLs. Geosynth. Int. 17 (5), 301–312.
Beddoe, R. a., Take, W.A., Rowe, R.K., 2011. Water-retention behavior of geosynthetic clay liners. J. Geotech. Geoenviron. Eng. 137, 1028–1038 (November).
Bouazza, A., Ali, M.A., Gates, W.P., Rowe, R.K., 2017. New insight on geosynthetic clay liner hydration: the key role of subsoils mineralogy. Geosynth. Int. 24 (2), 139–150.
Bouazza, A., Singh, R.M., Rowe, R.K., Gassner, F., 2014. Heat and moisture migration in a geomembrane–GCL composite liner subjected to high temperatures and low vertical stresses. Geotext. Geomembranes 42 (5), 555–563.
Campanella, R.G., Mitchell, J.K., 1968. Influence of temperature variations on soil behavior. In: Journal of Soil Mechanics & Foundations Div.
Campbell, G.S., Smith, D.M., Teare, B.L., 2007. Application of a dew point method to obtain the soil water characteristic. In: Experimental Unsaturated Soil Mechanics, vol. 112. Springer Berlin Heidelberg, Berlin, Heidelberg, pp. 71–77.
Casini, F., Vaunat, J., Romero, E., Desideri, A., 2012. Consequences on water retention properties of double-porosity features in a compacted silt. Acta Geotechnica 7 (2), 139–150.
Fredlund, D.G., Xing, A., 1994. Equations for the soil-water characteristic curve. Can. Geotech. J. 31 (4), 521–532.
Gallipoli, D., 2012. A hysteretic soil-water retention model accounting for cyclic variations of suction and void ratio. Geotechnique 62 (7), 605–616.
Gallipoli, D., Wheeler, S.J., Karstunen, M., 2003. Modelling the variation of degree of saturation in a deformable unsaturated soil. Géotechnique 53 (1), 105–112.
Gao, H., Shao, M., 2015. Effects of temperature changes on soil hydraulic properties. Soil Tillage Res. 153, 145–154.
Grant, S.A., Salehzadeh, A., 1996. Calculation of temperature effects on wetting coefficients of porous solids and their capillary pressure functions. Water Resour. Res. 32 (2), 261–270.
Hanson, J.L., Risken, J.L., Yesiller, N., 2013. Moisture-suction relationships for geosynthetic clay liners. In: Proceedings of the 18th International Conference on Soil Mechanics and Geotechnical Engineering, pp. 3025–3028 (Paris, France).
Hu, R., Chen, Y.-F., Liu, H.-H., Zhou, C.-B., 2013. A water retention curve and unsaturated hydraulic conductivity model for deformable soils: consideration of the change in pore-size distribution. Geotechnique 63 (16), 1389–1405.
Huang, Q., Zhao, C., Cai, G., 2016. The formulation of the water retention curve with deformation and hysteresis. In: Chen, Z., Wei, C., Sun, D., Xu, X. (Eds.), Unsaturated Soil Mechanics - from Theory to Practice. Proceedings of the 6th Asia Pacific Conference on Unsaturated Soils. CRC Press, Guilin, China, pp. 525–530.
IAPWS R7-97, 2012. Revised Release on the IAPWS Industrial Formulation 1997 for the Thermodynamic Properties of Water and Steam.
ISO 9863-1, 2016. Geosynthetics — Determination of Thickness at Specified Pressures. BSI Standards Publication, London, UK British Standards.
Jafari, N.H., Stark, T.D., Rowe, R.K., 2014. Service life of HDPE geomembranes subjected to elevated temperatures. J. Hazard. Tox. Radioact. Waste 18 (1), 16–26.
Khalili, N., Habte, M.A., Zargarbashi, S., 2008. A fully coupled flow deformation model for cyclic analysis of unsaturated soils including hydraulic and mechanical hystereses. Comput. Geotech. 35 (6), 872–889.
Leblanc, J., Akbarzadeh, A., Andrews, J., Lu, H., Golding, P., 2011. Heat extraction methods from salinity-gradient solar ponds and introduction of a novel system of heat extraction for improved efficiency. Sol. Energy 85 (12), 3103–3142.
Leong, E.C., Tripathy, S., Rahardjo, H., 2003. Total suction measurement of unsaturated

soils with a device using the chilled-mirror dew-point technique. Geotechnique 53 (2), 173–182.
Lloret, A., Alonso, E., 1980. Consolidation of unsaturated soils including swelling and collapse behaviour. Geotechnique 30 (4), 449–477.
Lloret, A., Alonso, E.E., 1985. State surfaces for partially saturated soils. In: In Proceedings of the 11th International Conference on Soil Mechanics and Foundation Engineering. Calif, San Francisco,, pp. 557–562.
Lu, Y., Abuel-Naga, H., Bouazza, A., 2017. Water retention curve of GCLs using a modified sample holder in a chilled-mirror dew-point device. Geotext. Geomembranes 45 (1), 23–28.
Olivella, S., Carrera, J., Gens, a., Alonso, E.E., 1994. Nonisothermal multiphase flow of brine and gas through saline media. Transport Porous Media 15 (3), 271–293.
Petrov, R.J., Rowe, R.K., 1997. Geosynthetic clay liner (GCL) - chemical compatibility by hydraulic conductivity testing and factors impacting its performance. Can. Geotech. J. 34 (6), 863–885.
Philip, J.R., de Vries, D. a., 1957. Moisture movements in porous materials under temperature gradients. Trans. Am. Geophys. Union 38 (2), 222–232.
Rajesh, S., Khan, V., 2018. Applied Clay Science Characterization of water sorption and retention behavior of partially saturated GCLs using vapor equilibrium and fi lter paper methods. Appl. Clay Sci. 157 (February), 177–188.
Risken, J.L., 2014. Development and Use of Moisture-suction Relationships for Geosynthetic Clay Liners. California Polytechnic State University, San Luis Obispo.
Risken, J.L., Hanson, J.L., Yesiller, N., 2016. Estimation of engineering behavior of geosynthetic clay liners using moisture-suction relationships. Jpn. Geotech. Soc. Spec. Publ. 2 (69), 2373–2378.
Romero, E., Gens, A., Lloret, A., 2001. Temperature effects on the hydraulic behaviour of an unsaturated clay. Geotech. Geol. Eng. 19 (3/4), 311–332.
Romero, E., Lloret, A., Gens, A., 1995. Development of a new suction and temperature controlled oedometer cell. In: Proceedings of the First International Conference on Unsaturated Soils, UNSAT'95, pp. 553–559 (Paris, France).
Roshani, P., Sedano, J.Á.I., 2016. Incorporating temperature effects in soil-water characteristic curves. Indian Geotech. J. 46 (3), 309–318.
Rouf, M.A., Bouazza, A., Singh, R.M., Gates, W.P., Rowe, R.K., 2016. Water vapour adsorption and desorption in GCLs. Geosynth. Int. 23 (2), 86–99.
Rouf, M.A., Singh, R., Bouazza, A., Gates, W., Rowe, R., 2014. Evaluation of a geosynthetic clay liner water retention curve using vapour equilibrium technique. In: Unsaturated Soils: Research & Applications, vol. 2. CRC Press, pp. 1003–1009.
Rowe, R.K., 2012. Short- and long-term leakage through composite liners. The 7th Arthur Casagrande Lecture. Can. Geotech. J. 49 (2), 141–169.
Rowe, R.K., Quigley, R., Brachman, R., Booker, J.R., 2004. Barrier Systems for Waste Disposal Facilities. CRC Press, London.
Rowe, R.K., Shoaib, M., 2017. Effect of brine on long-term performance of four HDPE geomembranes. Geosynth. Int. 24 (5), 508–523.
Rowe, R.K., Shoaib, M., 2018. Durability of HDPE geomembrane seams immersed in brine for three years. J. Geotech. Geoenviron. Eng. 144 (2), 1–12.
Russell, A.R., 2014. How water retention in fractal soils depends on particle and pore sizes, shapes, volumes and surface areas. Geotechnique 64 (5), 379–390.
Seiphoori, A., Laloui, L., Ferrari, A., Hassan, M., Khushefati, W.H., 2016. Water retention and swelling behaviour of granular bentonites for application in Geosynthetic Clay Liner (GCL) systems. Soils Found. 56 (3), 449–459.
Sheng, D., Fredlund, D.G., Gens, A., 2008. A new modelling approach for unsaturated soils using independent stress variables. Can. Geotech. J. 45 (4), 511–534.
Sheng, D., Zhou, A.-N., 2011. Coupling hydraulic with mechanical models for unsaturated soils. Can. Geotech. J. 48 (5), 826–840.
Southen, J.M., Rowe, R.K., 2005. Laboratory investigation of geosynthetic clay liner desiccation in a composite liner subjected to thermal gradients. J. Geotech. Geoenviron. Eng. 131 (7), 925–935.
Southen, J.M., Rowe, R.K., 2007. Evaluation of the water retention curve for geosynthetic clay liners. Geotext. Geomembranes 25 (1), 2–9.
Tarantino, A., 2009. A water retention model for deformable soils. Geotechnique 59 (9), 751–762.
van Genuchten, M.T., 1980. A closed-form equation for predicting the hydraulic conductivity of unsaturated soils. Soil Sci. Soc. Am. J. 44 (5), 892.
Wang, Y., Ma, J., Guan, H., 2016. A mathematically continuous model for describing the hydraulic properties of unsaturated porous media over the entire range of matric suctions. J. Hydrol. 541, 873–888.
Ye, W., Chen, B., Chen, Y., 2009. Effect of temperature on soil-water characteristics and hysteresis of compacted Gaomiaozi bentonite. J. Cent. S. Univ. Technol. 16, 821–826.
Yeşiller, N., Hanson, J.L., Liu, W.-L., 2005. Heat generation in municipal solid waste landfills. J. Geotech. Geoenviron. Eng. 131 (11), 1330–1344.
Zhou, A.-N.N., Sheng, D., Li, J., 2014. Modelling water retention and volume change behaviours of unsaturated soils in non-isothermal conditions. Comput. Geotech. 55, 1–13.
Zhou, C., Ng, C.W.W., 2014. A new and simple stress-dependent water retention model for unsaturated soil. Comput. Geotech. 62, 216–222.